Science of the Total Environment 650 (2019) 2685–2696

Contents lists available at ScienceDirect

Science of the Total Environment

journal homepage: www.elsevier.com/locate/scitotenv

# Impacts of climate change on streamflow and sediment concentration under RCP 4.5 and 8.5: A case study in Purna river basin, India

Aditya P. Nilawar *, Milind L. Waikar

*Department of Civil Engineering, Shri Guru Gobind Singhji Institute of Engineering and Technology (SGGS IE &T), Nanded 431605, India*

## HIGHLIGHTS

- Future climate data were generated by three climate model for RCP 4.5 and 8.5.
- Projected precipitation and temperature indicated an increasing trend in all season.
- Streamflow and sediment concentration were found to increase more under RCP 8.5.
- Stream contributed more than 50% of sediment concentration by eroding stream bank.

## GRAPHICAL ABSTRACT

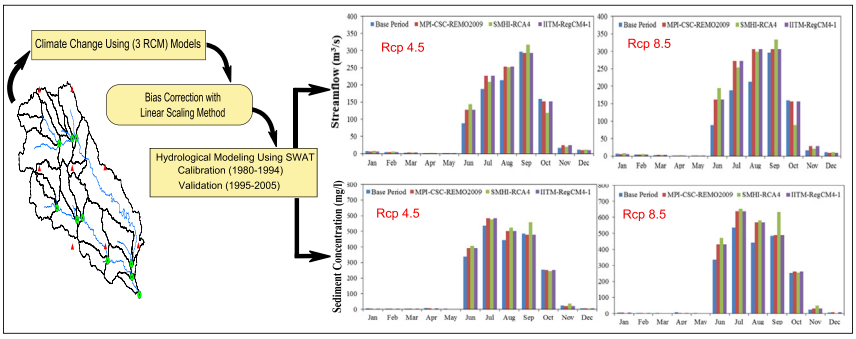


## ARTICLE INFO

*Article history:*
Received 31 May 2018
Received in revised form 22 September 2018
Accepted 26 September 2018
Available online 4 October 2018

Editor: Damia Barcelo

*Keywords:*
Climate change
RCM
SWAT
Streamflow
Sediment concentration

## ABSTRACT

Climate change has a significant effect on various hydrological processes in a large river basin. The assessment of these processes is also useful for water resource management and long-term sustainability of any hydrological project. In this study, an attempt is made to quantify the effects of climate change on streamflow and sediment concentration in the Purna river basin, India. Three Regional Circulation Models (RCMs) with two Representative Concentration Pathways (RCPs) 4.5 and 8.5 for the four future periods of P1 (2009–2031), P2 (2032–2053), P3 (2054–2075) and P4 (2076–2099) are considered. Differences in scenarios are compared with the base period 1980–2005. The SWAT is used on monthly basis for the period 1980 to 2005 with calibration period 1980 to 1994 and validation period 1995 to 2005. The projected precipitation and temperature show a significant increasing trend compared to the baseline condition for both RCPs. Similarly, the average monthly streamflow is projected to increase by 24.47 to 115.94 $m^3/s$ whereas average monthly sediment concentration by 32.58 to 162.96 mg/l under RCP 4.5 and 8.5. In particular, streamflow and sediment are expected to increase significantly from June to September at the outlet of the basin. The study results give insight into future hydrological scenarios which will be useful for policy makers to implement effective water resource strategies.

© 2018 Elsevier B.V. All rights reserved.

## 1. Introduction

The accumulation of greenhouse gases (GHG) in the environment is a major concern for global climate changes. These changes or alterations may, therefore, influence natural water resources (Arnell, 1999). According to the Intergovernmental Panel on Climate Change (IPCC) report, increase in temperature and variability of precipitation will

* Corresponding author at: Department of Civil Engineering, SGGG IE & T, Nanded, India.
*E-mail addresses:* nilawaraditya@sggs.ac.in (A.P. Nilawar), mlwaikar@sggs.ac.in (M.L. Waikar).

https://doi.org/10.1016/j.scitotenv.2018.09.334
0048-9697/© 2018 Elsevier B.V. All rights reserved.

attribute significantly to water-related risks such as flood and drought (Lindner et al., 2010). Especially, developing country like India is now facing severe climate change effects on water and agriculture sector. Therefore, the spatiotemporal response information on water resources to the climate change is important to figure out future water availability and sustainable water management plans. Gosain et al. (2006) assessed the impact of climate change on 12 Indian river basins for present and future greenhouse gas with HadRM2 climate data. The initial investigation predicted the occurrence of severe flood and drought during the 21st century.

Presently, it is of great importance to assess the influence of climate change on the regional water resources. Various factors including evapotranspiration, infiltration, and surface runoff also get affected due to climate change (Di Baldassarre et al., 2011; Joo et al., 2017). Furthermore, continuous progression in climate change may impact the water quality by altering the hydrological component. The effect of climate change on basin hydrology is normally assessed by characterizing climate change scenario to a hydrological model that is based on the futuristic greenhouse gas emission (Anand et al., 2018; Hosseini et al., 2015; Johnston and Smakhtin, 2014). Modeling streamflow is crucial for sediment concentration in the channel whereas peak streamflow rate is essential for the hydraulic structure design, flood protection and watershed management practices (Delpla et al., 2009; Routschek et al., 2014; Zhao et al., 2018). The conventional methods of measuring hydrological parameter are monotonous and time-consuming so it is desirable to use recently developed Remote Sensing (RS) and GIS-based hydrological model. Recent studies suggested that SWAT is widely used as a resourceful model to assess environmental and hydrological changes with fluctuating land type and weather conditions (Malagó et al., 2017). In addition, the output variables incorporated in the SWAT are found to address various water-related processes in the watershed (Bharati et al., 2012; Dahal et al., 2016). These models are postulated as a system based hydrological model to determine land use land cover impact and management practice on the river basin or watershed (Zhang et al., 2007). Ficklin et al. (2009) assessed the climate change impact in the highly agricultural area using the semi-distributed SWAT model in California (USA). The study results highlighted that an increase in concentration $CO_2$ have a remarkable effect on streamflow, evaporation and water yield. In a similar investigation, Murty et al. (2014) employed SWAT to predict water balance component in Ken basin, India. The successful application for hydrological evaluation was carried out for 25 years (1985–2009).

The IPCC defines a series of RCP scenarios (2.5, 4.5, 6 and 8.5) for future climate projection based on Coupled Model Intercomparison Project (CMIP5) (Tan et al., 2014; Van Vuuren et al., 2011). These four RCPs incorporate one alleviation scenarios priming a low driving level (RCP2.6), two stabilization scenarios (RCP4.5 and RCP6), and, one scenario with high greenhouse gas emissions (RCP8.5). These scenarios are evolved based on the driving force such as the growth of population, socio-economic development and GHG (McGuire et al., 2001; Willems and Vrac, 2011). As per the IPCC report, the global temperature may increase by 1 °C to 5 °C by the end of the century. Climate scenarios

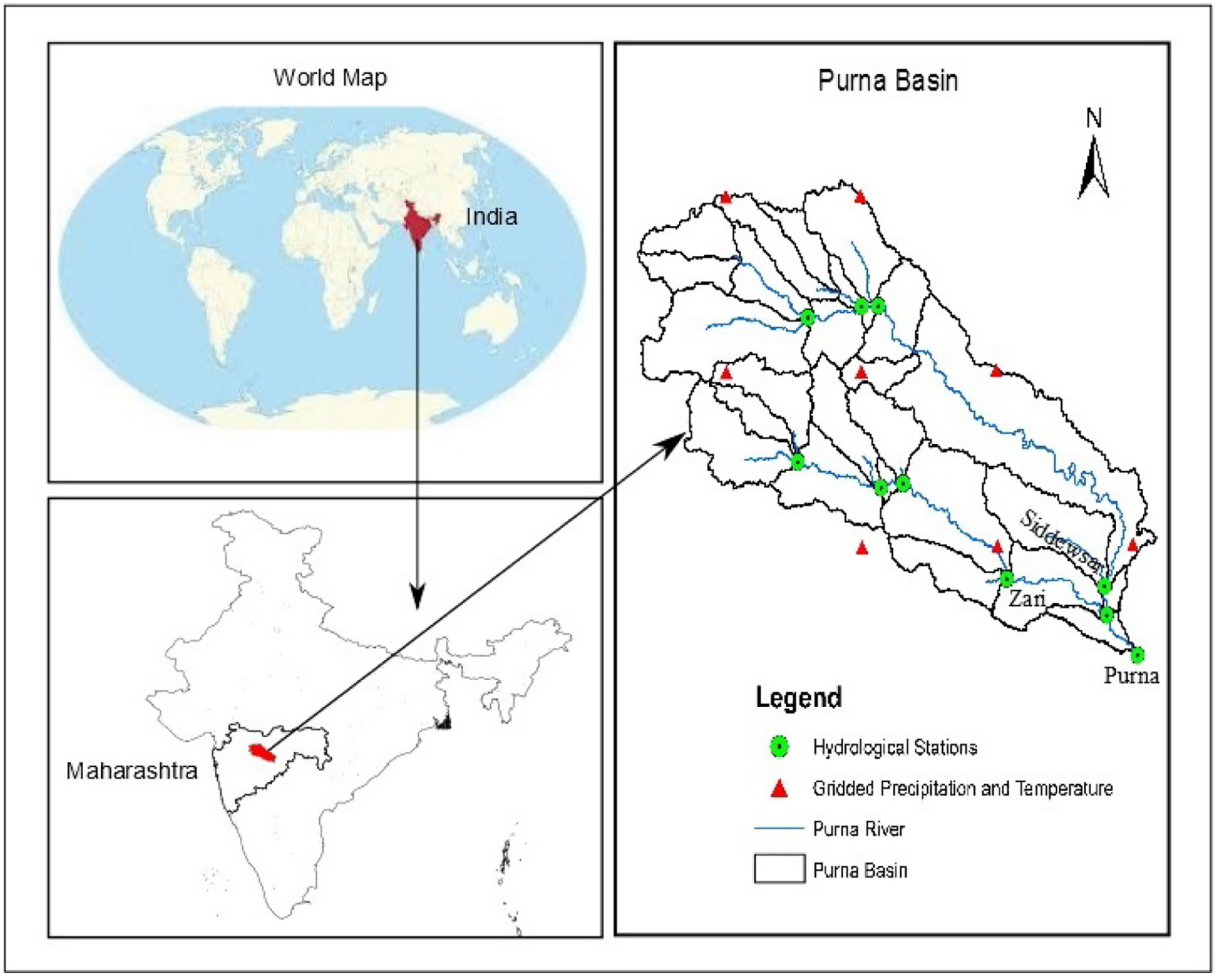


**Fig. 1.** Location map of Purna river basin with precipitation, temperature and hydrological station in India.

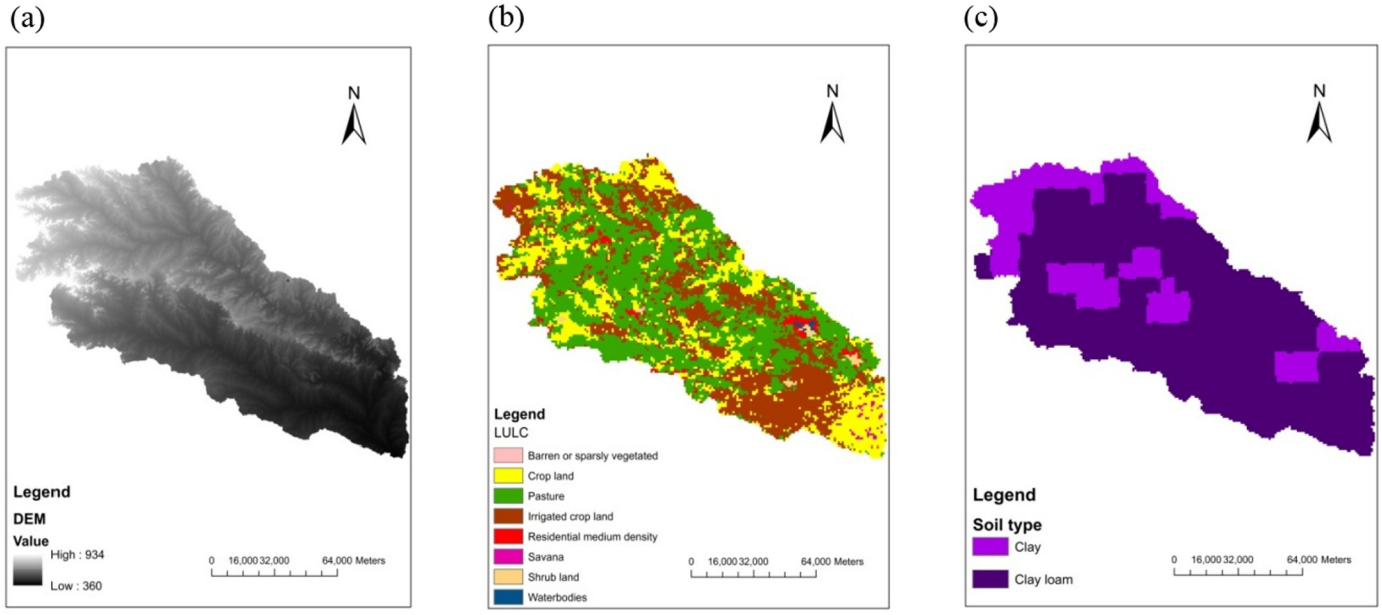


**Fig. 2.** Spatial input details used in the SWAT (**a**) DEM (30 m resolution) ranges from 360 m to 934 m; (**b**) LULC classification; (**c**) Soil classification.

for both Global climate model (GCM) or simple analog models are often adapted to examine the effect of climate change on hydrology (Fereidoon and Koch, 2018). However, their spatial resolutions are excessively coarse for regional climate study (Abdo et al., 2009; Christensen et al., 2004). Hence, fine downscaling technique either through statistical or dynamic regional climate models is needed. Min et al. (2011) demonstrated that human influence increments in greenhouse gases contributed to an escalation of extreme precipitation over the Northern Hemisphere. Changes in hydrological parameters were noted at a worldwide scale with considerable variability in events of flood and drought. Bajracharya et al. (2018) projected change in the hydrological regime under RCP 4.5 and RCP 8.5 scenario in Kaligandaki basin, Nepal. It was seen that increase in average annual temperature and precipitation by end of the 21st century may lead to significant change in water balance and hydrological regime with about 50% increment in the discharge of the basin. Ligaray et al. (2015) examined the hydrological responses under several climate sensitive and greenhouse gas emission scenarios in the Chao Phraya river, Thailand. The study was focused on a framework for peak flow that can be directed to control nonpoint sources during wet seasons and revealed that an increase in $CO_2$ accumulation leads to a dramatic change in streamflow. Cousino et al. (2015) evaluated the effect of climate change on magnitude and timing of sediment and nutrient delivery in the Maumee river basin, USA. A SWAT was incorporated with CMIP 5 climate data. The results revealed a significant effect of climate change on sediment yield in the river basin. Li and Gao (2015) investigated the climate change effect on water resource under two emission scenarios in the Songhua river basin, China. The study was carried out for the period from 2020 to 2049 with downscaled climate data. The results indicate a change in temperature and precipitation has a significant effect on streamflow. There are limited studies addressing the climate change analysis using RCM on streamflow and sediment concentration in the region. However most of the studies have used coarse resolution GCM data which are not preferred for hydrological modeling.

As discussed above, to obtain reasonably accurate streamflow and sediment concentration projection is the major scientific problem in

**Table 1**
The sensitive parameter for streamflow and sediment concentration with fitted values for the calibration.

| Parameter | Parameter name | Initial range | t-Stat | p-Value | Rank | Fitted values |
|---|---|---|---|---|---|---|
| CN2 | SCS runoff curve number | −0.2 to 0.2 | −7.005 | 0.000 | 4 | −0.14 |
| ALPHA_BF | Base flow alpha factor | 0 to 1 | 8.883 | 0.000 | 3 | 0.35 |
| GW_DELAY | Groundwater delay time | 30 to 450 | −3.585 | 0.000 | 7 | 74 |
| GWQMN | Threshold depth of water in shallow aquifer for return flow to occur | 0 to 2 | −0.366 | 0.713 | 17 | 0.52 |
| GW_REVAP | Groundwater revap. coefficient | 0 to 0.3 | 1.832 | 0.067 | 9 | 0.2 |
| ESCO | Soil evaporation compensation factor | 0.5 to 1 | −2.976 | 0.002 | 8 | 0.81 |
| CH_N2 | Manning's n value for main channel | 0 to 0.3 | −4.691 | 0.000 | 6 | 0.04 |
| CH_K2 | Effective hydraulic conductivity in the main channel | 5 to 130 | −6.678 | 0.000 | 5 | 4.32 |
| ALPHA_BNK | Base flow alpha factor for bank storage | 0 to 1 | 10.010 | 0.000 | 1 | 0.41 |
| SOL_AWC | Soil available water storage capacity | −0.2 to 0.5 | 1.822 | 0.068 | 10 | 0.42 |
| SOL_K | Soil conductivity | −0.8 to 0.8 | 9.800 | 0.000 | 2 | −0.06 |
| SOL_BD | Moist bulk density of first soil layer | −0.5 to 0.6 | −1.039 | 0.298 | 11 | −0.16 |
| USLE_C.plant | USLE cover factor | −2 to 2 | 0.303 | 0.768 | 19 | 1.03 |
| CH_COV2 | Channel cover factor | −0.14 to 0.35 | −0.337 | 0.743 | 18 | 0.34 |
| USLE_K | USLE equation soil erodibility K factor | 0.10 to0.40 | 0.390 | 0.705 | 16 | 0.21 |
| LAT_SED | Sediment concentration in lateral and groundwater flow | 10 to133 | 0.409 | 0.691 | 15 | 90.34 |
| CH_COV1 | Channel erodibility factor | 0.13 to0.45 | 0.596 | 0.565 | 14 | 0.43 |
| SPCON | Linear parameter for calculating sediment re-entered in channel sediment routing | 0.002 to 0.004 | 0.685 | 0.510 | 13 | 0.003 |
| SPEXP | Exponent parameter for calculating sediment re-entered in channel sediment routing | 1.24 to 1.74 | −0.809 | 0.438 | 12 | 1.70 |

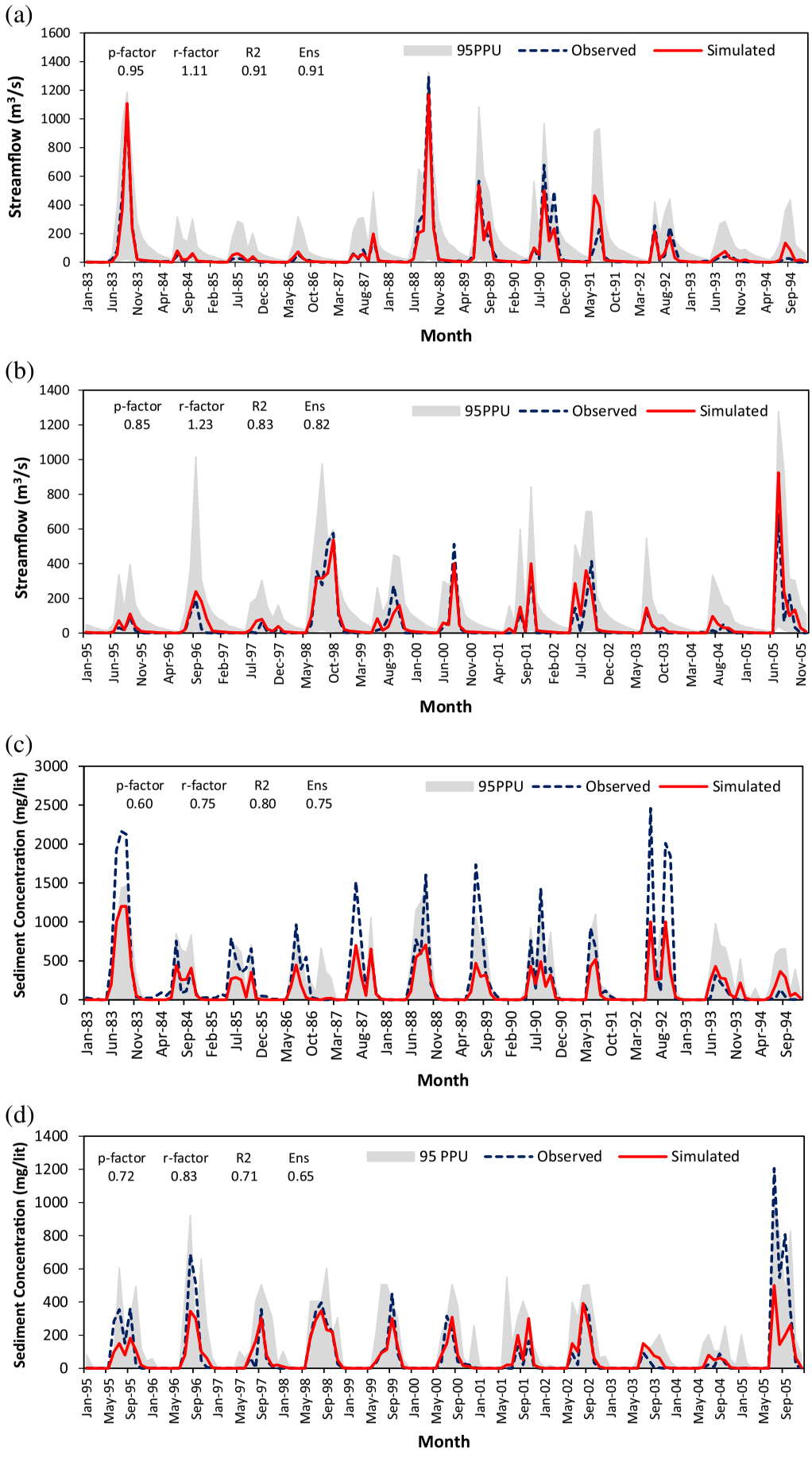
(a)
p-factor 0.95
r-factor 1.11
R2 0.91
Ens 0.91
95PPU
Observed
Simulated
Streamflow (m³/s)
Month
(b)
p-factor 0.85
r-factor 1.23
R2 0.83
Ens 0.82
95PPU
Observed
Simulated
Streamflow (m³/s)
Month
(c)
p-factor 0.60
r-factor 0.75
R2 0.80
Ens 0.75
95PPU
Observed
Simulated
Sediment Concentration (mg/lit)
Month
(d)
p-factor 0.72
r-factor 0.83
R2 0.71
Ens 0.65
95 PPU
Observed
Simulated
Sediment Concentration (mg/lit)
Month

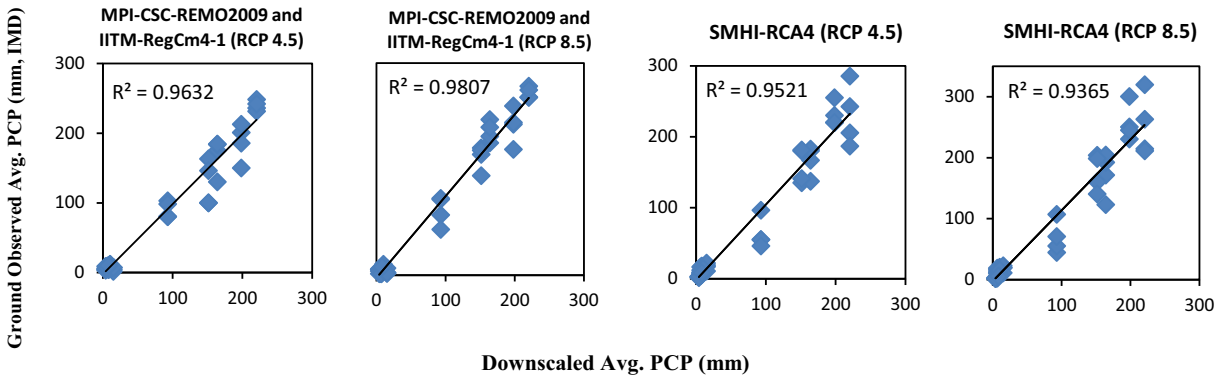


**Fig. 4.** Scatter plot of ground observed average monthly precipitation against downscaled average precipitation.

hydrology and therefore the orientation of the present study is to understand the environmental and hydrological basin response with respect to landuse, soil, topography and climatic conditions. The novelty of the study is to use of various RCMs to cover a wide range of potential outcomes in future climate and adapt comparatively simple bias correction technique (linear scaling) in Purna river basin including hydrological analysis with SWAT. The primary objectives are: (1) To quantify the impact of climate change on streamflow and sediment concentration in the Purna river basin using semi-distributed SWAT. (2) To identify future temperature and precipitation change for period P1 (2009–2031), P2 (2032–2053), P3 (2054–2075) and P4 (2076–2099) under RCP 4.5 and RCP 8.5 emission scenarios. RCP 4.5 and RCP 8.5 are selected in this study to represent the possible future by 2099 under medium stabilization and very high baseline emission scenarios respectively.

## 2. Materials and methods

### 2.1. Study area

The Purna river originates from the Ajanta hill ranges is a significant left bank tributary of the Godavari river. The river flows across Aurangabad, Buldana, Jalna, Hingoli and Parbhani districts of Maharashtra state as shown in Fig. 1. The river length is about 373 km before confluences in Godavari river and covers an area of 15,579 km$^2$. The basin geographical boundary lies between 75°12′25″ E to 77°03′27″ E longitude and 20° 21′38″ N to 19°10′19″ N latitudes and elevation ranges from 360 m to 934 m above mean sea level. In general, the average annual rainfall received by the river basin is 800 mm out of which more than 90% is contributed by South West monsoon from June to September. The average minimum and maximum temperature in the basin varies from 14.5 °C (December to January) to 35.5 °C (May) respectively. The principal tributaries of the Purna river are Kelana, Damna, Lendi, Anjana, Girija and Dudhana. The longest tributary of Purna is Dudhana river and comprises of Yeldari and Siddheshwar dams.

### 2.2. Model input data

The main spatial inputs required for the SWAT processing are Digital Elevation Model (DEM), soil and land use. In the present study, Shuttle Radar Topography Mission (SRTM) DEM of 30 m resolution is used to calculate the watershed parameters concerning the slope length, flow accumulation, direction and stream network. The DEM (Fig. 2 a) is obtained from the United State Geographical Survey (USGS) (https://earthexplorer.usgs.gov/). The LULC is prepared from an IRS-P6 LISS-III (Linear Image Self Scanning) 2013 year image. Further, the image is classified into land use classes with observed field data in ERDAS IMAGINE 2015. It can be observed from Fig. 2 (b) that the cropland is the dominant land cover in the basin and covered about 55% of the total basin area. Soil data is obtained by downloading the attributes from FAO global soil data (1:50000) (http://www.fao.org). Moreover, data based on the soil properties such as texture, soil water content, hydrological soil group, depth of soil, bulk density, and organic carbon content is modified in the required format. From Fig. 2 (c), it is noticed that the prevailing type of soil in the study area are chromic vertisols and vertic cambisols (clay and clay loam). The SWAT requires daily precipitation, temperature, wind speed, solar radiation and relative humidity data. The daily gridded precipitation and temperature for the duration of 1980 to 2005 for 26 years are collected from the Indian Metrological Department (IMD). The rest of the parameters are estimated internally by SWAT weather generator. The monthly streamflow and sediment for the period 1980 to 2005 at the gauge site is acquired from India-WRIS project (http://www.india-wris.nrsc.gov.in). As the study area is located in the South Asia region of CORDEX, three RCM CMIP 5 models coupled with RCP 4.5 and RCP 8.5 are used for the climate study. Climate data, precipitation and temperature from climate model (MPI-CSC-REMO2009, SMHI-RCA4 and IITM-RegCM4-1) are downloaded for the period 2006 to 2099 (https://esgfdata.dkrz.de/search/cordex-dkrz).

### 2.3. SWAT model

The significant parameters involved in the model development are hydrology, climate change, water quality, land practices, agriculture, vegetation growth and stream routing. In the initial stage of methodology involves demarcation of basin or watershed. The demarked basin is further sub-classified as HRU with a unique grouping of landuse, slope and soil (Romagnoli et al., 2017). Hydrological parameter simulation at each HRU is performed by employing following water balance equation:

$$SW_f = SW_i + \sum \left[R_d - Q_{sur} - ET_v - W_{seep} - Q_{gwt}\right] \quad (1)$$

where, $SW_f$ is the total soil water content (mm), $SW_i$ is the primary soil water content (mm), precipitation and the total surface runoff is given by $R_d$ (mm) and $Q_{sur}$ (mm). The evapotranspiration, percolation and return flow are given by $ET_v$ (mm), $W_{seep}$ (mm) and $Q_{gwt}$ (mm) (Chaibou Begou et al., 2016; Shi et al., 2013).

**Fig. 3.** Monthly observed and simulated streamflow: (a) calibration (1983–1994) (b) validation (1995–2005), sediments concentration: (c) calibration (1983–1994) (d) validation (1995–2005).

The streamflow, infiltration, and canopy storage are estimated by the Soil Conservation Services Curve Number method (SCS-CN). The modified ratio method or SCS TR-55 method is utilized to estimate the stream peak flow while a kinematic storage routing technique is used to simulate lateral flow (Gupta et al., 2011; Williams et al., 2011). Moreover, shallow aquifer is employed to determine the return flow stream in the Purna river basin. In the present study, the Hargreaves method has been selected for the estimation of evapotranspiration for balancing the mass components for the process of calibration. In SWAT, the channel routing is determined using the Muskingum method whereas the empirical approach is adopted to analyze the groundwater. The output of SWAT comprises water balance component for each watershed and flows at the outlet point.

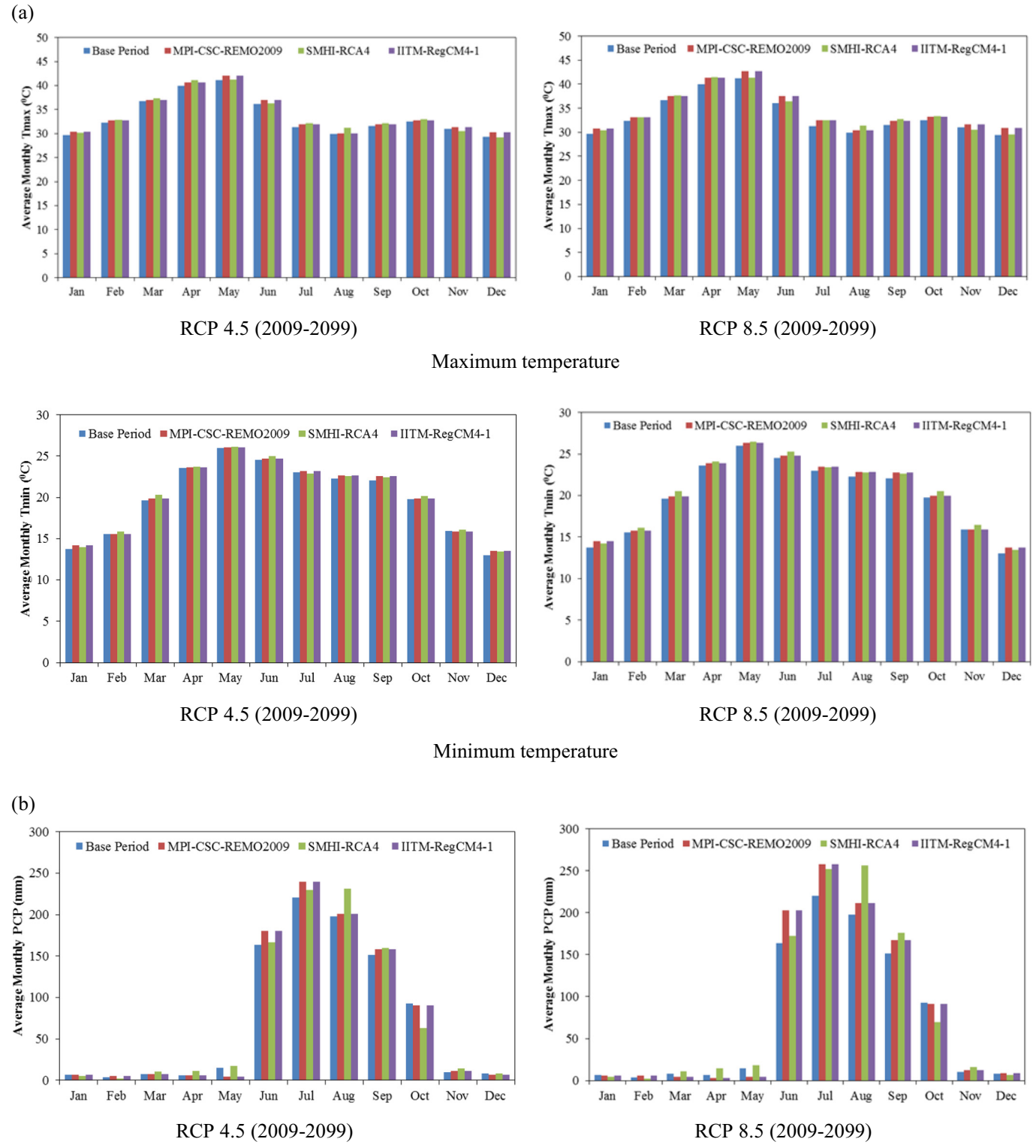


**Fig. 5.** Average monthly change in (a) maximum and minimum temperature (b) precipitation (RCP 4.5 and RCP 8.5) comparison with the base period for MPI-CSC-REMO2009, SMHI-RCA4 and IITM-RegCM4-1 model.

The SWAT uses Modified Universal Soil Loss Equation (MUSLE) to determine the sediment concentration at HRU level (Vigiak et al., 2017; Zeiger and Hubbart, 2016) and expressed as follows:

$$P_s = 11.8\ (Q.P_{peak}.A)^{0.56} K.C.P.LS.CF \quad (2)$$

where, $P_s$ is the sediment yield on a given day (metric tons), $Q$ is the surface runoff volume in ($m^3$), $p_{peak}$ is the peak runoff rate ($m^3$/s), $A$ is the HRU area (ha), $K$ is USLE soil erodibility factor, $C$ is USLE cover and management factor, $P$ is USLE erosion control practice factor, $LS$ is USLE slope and gradient factor and $CF$ is coarse fragment factor.

Finally, the SWAT performance is assessed on the basis of the statistical relation between observed and simulated results. The coefficient of determination ($R^2$) and Nash-Sutcliffe efficiency ($E_{NS}$) are the most frequently used statistical indices in the calibration and validation process (Meng et al., 2018) and expressed as:

$$R^2 = \frac{\left[\sum_{i=1}^{n}\left(Q_i-\overline{Q}\right)\left(S_i-\overline{S}\right)\right]^2}{\left[\sum_{i=1}^{n}\left(Q_i-\overline{Q}\right)^2\right]\left[\sum_{i=1}^{n}\left(S_i-\overline{S}\right)^2\right]} \quad (3)$$

$$E_{NS} = 1-\left[\frac{\sum_{i=1}^{n}(Q_i-S_i)^2}{\sum_{i=1}^{n}\left(Q_i-\overline{Q}\right)^2}\right] \quad (4)$$

where, $Qi$ and $S_i$ are measured and simulated values,$\overline{Q}$ and $\overline{S}$ are mean measured and simulated values.

### 2.4. Climate change projections and bias correction

In the present study, three RCM (MPI-CSC-REMO2009, SMHI-RCA4 and IITM-RegCM4-1) models are used which contains high-resolution daily temperature and precipitation for South Asia domain. The climate forecasting for the period 2006 to 2099 is analyzed under the RCP 4.5 and RCP 8.5. The RCP 4.5 considered carbon emission around 650 ppm and RCP 8.5 around 1370 ppm. Although these RCMs have good results on large scale, it contains some systematic error which cannot be directly used for model simulation. Hence, some bias correction techniques are required to remove these errors. In this study, linear scaling method is used to remove biases from RCMs (Lenderink et al., 2007; Teutschbein and Seibert, 2012). This method depends on the difference between monthly observed and simulated values. Further, these differences are implemented to simulated climate data for obtaining bias corrected variable. However, multiplicative and additive corrections are more appropriate for precipitation and maximum–minimum temperature. Following equations are used for linear scaling.

$$P\prime_{his}(d) = P_{his}(d) * \left[\frac{\mu_m(P_o(d))}{\mu_m(P_{his}(d))}\right] \quad (5)$$

$$P\prime_{prj}(d) = P_{prj}(d) * \left[\frac{\mu_m(P_o(d))}{\mu_m(P_{his}(d))}\right] \quad (6)$$

$$T\prime_{his}(d) = T_{his}(d) + \mu_m(T_o(d)) - \mu_m(T_{his}(d)) \quad (7)$$

$$T\prime_{prj}(d) = T_{prj}(d) + \mu_m(T_o(d)) - \mu_m(T_{his}(d)) \quad (8)$$

where, $P$–precipitation, $T$-temperature, $d$-day, $his$-RCM simulated 1980–2005, $prj$-RCM simulated 2006–2099, $o$-observed, $m$-within monthly interval.

## 3. Results

### 3.1. Sensitivity and uncertainty analysis

The global sensitivity of streamflow and sediment concentration parameter is performed using Latin hypercube against the objective

**Table 2**
Predicted relative change in monthly precipitation with the base period under RCP 4.5 and RCP 8.5 for (a) MPI-CSC-REMO2009 model and IITM-RegCM4-1 model (b) SMHI-RCA4 model.

(a)

| Month | Jan | Feb | Mar | Apr | May | Jun | Jul | Aug | Sep | Oct | Nov | Dec |
|---|---|---|---|---|---|---|---|---|---|---|---|---|
| Base period Precipitation (PCP) (mm) | | | | | | | | | | | | |
| (1983–2005) | 6.53 | 3.95 | 7.85 | 6.36 | 14.88 | 163.82 | 220.22 | 197.98 | 151.19 | 92.77 | 10.00 | 8.15 |
| Increase and decrease in Precipitation (PCP) (mm)RCP4.5 | | | | | | | | | | | | |
| P1 | −1.64 | 1.83 | −3.55 | 2.86 | −10.97 | 11.18 | 15.86 | 2.71 | 11.70 | −12.64 | 0.52 | −2.75 |
| P2 | 1.47 | −0.82 | 0.65 | −0.77 | −13.45 | 14.38 | 27.80 | 14.70 | −5.13 | −12.85 | 1.87 | −3.97 |
| P3 | 0.64 | 4.80 | 1.72 | −2.86 | −7.92 | 19.85 | 10.95 | −12.40 | 17.42 | 10.21 | 1.40 | −1.93 |
| P4 | 1.28 | 0.34 | −0.42 | −0.38 | −7.91 | 20.35 | 21.65 | 5.38 | 5.13 | 5.29 | 1.31 | 1.74 |
| Increase and decrease in Precipitation (PCP) (mm)RCP 8.5 | | | | | | | | | | | | |
| P1 | 1.48 | −1.99 | −4.88 | −3.68 | −11.13 | 23.10 | 31.26 | 15.16 | 19.60 | −7.84 | −1.92 | 0.54 |
| P2 | −2.80 | 3.68 | −0.29 | −3.02 | −4.98 | 32.16 | 47.06 | 41.12 | −10.41 | −28.29 | 2.66 | −1.73 |
| P3 | 3.47 | 4.67 | −5.15 | −2.60 | −11.85 | 56.18 | 31.33 | −20.29 | 28.81 | 15.80 | 4.07 | −0.58 |
| P4 | −4.72 | 1.76 | −2.03 | −4.64 | −12.45 | 45.35 | 41.56 | 17.86 | 25.27 | 14.28 | 5.31 | 3.38 |

(b)

| Month | Jan | Feb | Mar | Apr | May | Jun | Jul | Aug | Sep | Oct | Nov | Dec |
|---|---|---|---|---|---|---|---|---|---|---|---|---|
| Base period Precipitation (PCP) (mm) | | | | | | | | | | | | |
| (1983–2005) | 6.53 | 3.95 | 7.85 | 6.36 | 14.88 | 163.82 | 220.22 | 197.98 | 151.19 | 92.77 | 10.00 | 8.15 |
| Increase and decrease in Precipitation (PCP) (mm)RCP4.5 | | | | | | | | | | | | |
| P1 | 1.06 | −2.43 | −0.25 | 2.52 | 2.00 | 2.97 | −14.71 | 22.02 | −15.85 | 3.76 | 6.51 | 3.77 |
| P2 | −1.88 | −1.42 | 0.29 | 9.98 | 3.96 | 16.35 | −33.62 | 32.02 | 28.82 | −37.64 | 6.03 | −2.32 |
| P3 | −2.26 | −0.71 | 1.75 | 1.29 | −4.11 | 18.75 | 22.14 | 22.02 | 30.09 | −38.07 | −0.26 | −0.93 |
| P4 | −1.81 | −1.19 | 9.88 | 5.66 | 6.85 | −26.52 | 65.06 | 57.02 | −10.30 | −46.84 | 3.81 | −0.17 |
| Increase and decrease in Precipitation (PCP) (mm)RCP 8.5 | | | | | | | | | | | | |
| P1 | −0.47 | −2.06 | −0.52 | 5.94 | 4.45 | 7.56 | −5.97 | 32.31 | 9.06 | 14.29 | 10.16 | −1.87 |
| P2 | −4.32 | −2.15 | 0.86 | 9.37 | 4.91 | 28.25 | −9.03 | 52.45 | 52.68 | −48.17 | 9.11 | −1.55 |
| P3 | −2.32 | −2.01 | 3.96 | 4.38 | −4.10 | 40.46 | 42.52 | 47.02 | 47.14 | −37.74 | −1.31 | −0.23 |
| P4 | −1.57 | −1.03 | 9.26 | 12.62 | 7.78 | −40.88 | 99.14 | 102.02 | −11.01 | −22.38 | 6.00 | −2.43 |

function value (Arnold et al., 2012; Faramarzi et al., 2013). However, the average change in the objective functions is evaluated based on the consequential changes and sensitivity for each parameter, referred as the relative sensitivity (Baker and Miller, 2013; Xue et al., 2013). Thirteen parameters are considered for the sensitivity analysis and respective names are listed in Table 1. The significance of the parameter sensitivity is measured by considering the *p*-value and t-stat (Nilawar et al., 2017; Tuo et al., 2016). The parameters ALPHA_BNK, SOL_K, r_CN2, ALPHA_BF, and CH_K2 are observed as most sensitive in the Purna river basin. Consequently, the parameter, ALPHA_BNK is contributed to the main channel flow as a bank storage and observed to simulate the recession curve. However, the small fitted value of ALPHA indicates the steep recessions. During the calibration process, the sensitivity of the SOL_K is highly concerned with the existence of macrospores and rock fragments which are widely extended in the basin. The streamflow is found to be increased rapidly with increasing CN2 value. Additionally, it is noticed that higher CN2 value indicate water retained by the soil is less and higher occurrence of streamflow. A slow response of recharge to groundwater flow is observed with sensitivity parameter ALPHA_BF. The measure of the rate of water loss from the channel to groundwater is given by CH_K2, while a slow water displacement from stream bed to the subsurface of a stream is noticed with low values of CH_K2. In SUFI-2, the factors corresponding to the measured values are given as a p-factor of 1 and r-factor of zero (Yang et al., 2008). The results obtained from the simulations revealed that the values of the p-factor and the r-factor are 0.95 and 1.11 in the calibration period and for validation period values are 0.85 and 1.23. The percentage data being bracketed by 95 PPU (p-factor) for calibration and validation is high. However, during the calibration, it is found as 95% and for validation 85%. Similarly, for the sediment concentration, the p-factor is 0.60 and the r-factor is 0.75 in the calibration whereas for the validation it is 0.72 and 0.83 respectively. The obtained SWAT results reveal substantial uncertainties in the validation period.

### 3.2. Calibration and validation

The calibration is performed from 1980 to 1994 with an initial three years as a model warm-up. From the calibration results, it is noticed that simulated monthly streamflow values are matching with the observed values in the basis. The ($R^2$) and ($E_{NS}$) for streamflow calibration are obtained as 0.91 and 0.91 and for validation (1995 to 2005) as 0.83 and 0.82 respectively depicted in Fig. 3 (a) and (b). This indicates an acceptable correlation between the simulated and the observed values. On the other hand, the model performed equally well with observed sediment concentration in the basin which computes $R^2$ and $E_{NS}$ for calibration as 0.80 and 0.75 whereas for the validation it is 0.71 and 0.65 respectively depicted in Fig. 3 (c) and (d). Consequently, the assessment of runoff and sediment yield is performed for the total simulation period. The model considered the annual rainfall of 813.5 mm over Purna basin and partitions with water balance ratios as streamflow to precipitation of 20%, baseflow to the total flow of 32%, surface flow to total flow of 68%, deep recharge to precipitation of 2%, ET to precipitation of 44%. Thus, the estimated values of hydrology parameters are as follows: mean annual rainfall, 813.5 mm, PET is 1750.4 mm, evapotranspiration (ET) is 354.8 mm, PET is 1750.4 mm water yield is 178.88 mm, total

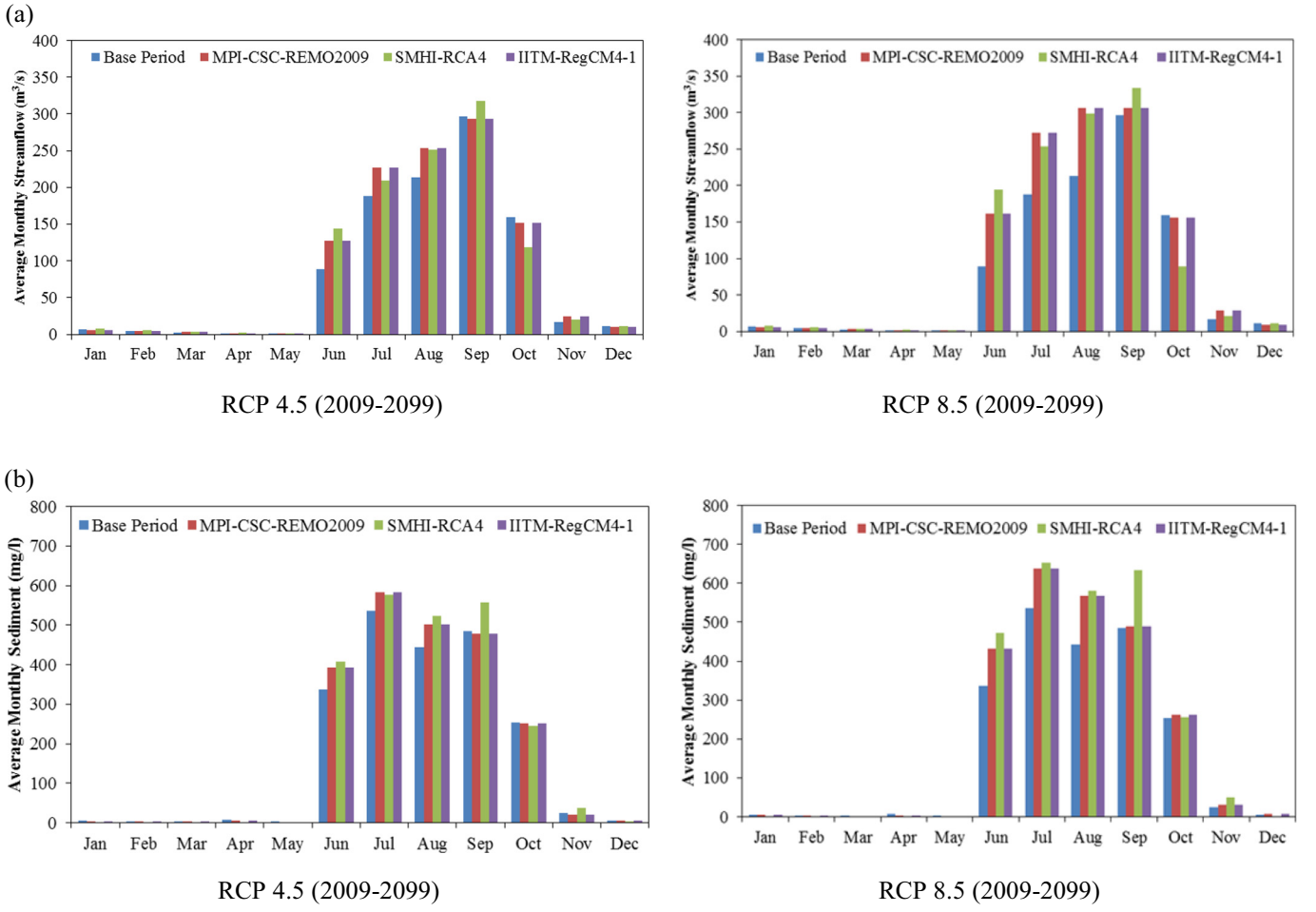


**Fig. 6.** Average monthly change in (a) streamflow (b) sediment concentration (RCP 4.5 and RCP 8.5) comparison with base period for MPI-CSC-REMO2009, SMHI-RCA4 and IITM-RegCM4-1 model.

aquifer recharge 347.39 mm and total sediment loading is 15.302 t/ha. However, the model efficiency and prediction capability can be improved with the enhancement of the data inputs.

### 3.3. Evaluation of downscaling

In this section the comparison of MPI-CSC-REMO2009, SMHI-RCA4 and IITM-RegCM4–1 models with corresponding IMD ground observation data is presented. The plots between observed and downscale average monthly precipitation (RCP4.5 and 8.5) are shown in Fig. 4. The coefficient of determination, $R^2$ values range from 0.93 to 0.98 thereby indicating better correspondence of downscaled and ground data.

### 3.4. Projected temperature and precipitation change

The precipitation, maximum and minimum temperature data are corrected using linear scaling for the RCM models MPI-CSC-REMO2009, SMHI-RCA4 and IITM-RegCM4-1. Further, this data is analyzed for the time period P1 (2009–2031), P2 (2032–2053), P3 (2054–2075) and P4 (2076–2099). The future bias corrected scenarios RCP 4.5 and RCP 8.5 is compared with the observed data from the base period 1980–2005. The average change in maximum and minimum temperature is shown in Fig. 5 (a). The projected maximum temperature ($t_{max}$) indicates a rise in temperature under all the scenarios. The $t_{max}$ projected for four future period ranges from 0.39–0.68 °C and 0.52–1.32 °C, under RCP 4.5 and RCP 8.5. Similarly, the rise in average minimum temperature ($t_{min}$) ranges from 0.17–0.38 °C and 0.3–0.63 °C. The comparison of RCP 4.5 and RCP 8.5 with respect to base period indicates significant increases in $t_{max}$ and $t_{min}$ under RCP 8.5. This infers that the Purna basin may face a hotter period in the future, particularly in dry month season (January to May).

The projected precipitation for both the RCPs is compared with the base period precipitation. The projected precipitation (PCP) for four future periods are increased by 1.28–6.90% (11.37 mm to 61.59 mm) and 4.90–10.61% (59.68 mm to 161.91 mm), under RCP 4.5 and RCP 8.5. The predicted precipitation is increased during the wet season from June to September especially for RCP 8.5. The monthly comparison between base period precipitation and future period precipitation is depicted in Fig. 5 (b). For models MPI-CSC-REMO2009, SMHI-RCA4 and IITM-RegCM4–1the precipitation ranges from P1 (−15.84 to 22.02 mm), P2 (−37.63 to 32.02 mm), P3 (−38.07 to 30.08 mm) and P4 (−46.84to 65.06 mm) under RCP 4.5.Whereas, for RCP 8.5 it ranges from P1 (−11.12 to 32.30 mm), P2 (−48.16 to 52.67 mm), P3 (−37.73 to 47.13 mm) and P4 (−40.88 to 102.02 mm). The negative value indicates a decrease in rainfall in the dry season and a positive value indicates an increase in rainfall, especially in wet season. It is observed that precipitation for the period (June to September) increased under all four periods and decreased in (January to May). It is also observed that, models MPI-CSC-REMO2009 and IITM-RegCM4–1 indicate similar results for monthly average temperature and precipitation. The details of monthly average changes are depicted in Table 2. Similar results were obtained by Das and Umamahesh (2016), wherein the study aim was to find out the spatial distribution of rainfall for 2.5, 4.5 and 8.5 scenarios in India. The downscaling technique was applied over 25 grid point in the basin. The study results indicate an increase in rainfall under all scenario for the future time period.

### 3.5. Climate change impact on streamflow

The calibrated SWAT model is interfaced with bias-corrected temperature and precipitation for future climate change scenario. The comparison in average monthly streamflow and base period is depicted in Fig. 6 (a). The streamflow projected for P1, P2, P3 and P4 periods are increased by 7.85–14.56% (77.61 to 143.98 $m^3/s$)

**Table 3**
Predicted relative change in monthly streamflow with the base period under RCP 4.5 and RCP 8.5 for (a) MPI-CSC-REMO2009 model and IITM-RegCM4-1 model (b) SMHI-RCA4 model.

(a)

| Month | Jan | Feb | Mar | Apr | May | Jun | Jul | Aug | Sep | Oct | Nov | Dec |
|---|---|---|---|---|---|---|---|---|---|---|---|---|
| Base period streamflow (B_flow) ($m^3/s$) | | | | | | | | | | | | |
| (1983–2005) | 6.34 | 4.43 | 2.76 | 1.27 | 0.44 | 88.68 | 187.77 | 213.38 | 296.73 | 159.23 | 16.16 | 11.05 |
| Increase and decrease in streamflow ($m^3/s$) under RCP4.5 | | | | | | | | | | | | |
| P1 | −0.66 | −0.54 | −0.43 | −0.28 | −0.19 | 24.47 | 50.64 | 34.14 | −5.263 | −11.21 | 3.71 | −2.32 |
| P2 | −0.48 | −0.32 | −0.33 | −0.17 | −0.14 | 43.02 | 41.11 | 37.22 | 3.39 | −37.84 | 6.13 | −2.36 |
| P3 | 0.32 | 1.55 | 1.04 | 0.21 | −0.06 | 41.35 | 30.11 | 46.42 | 9.05 | −16.02 | 18.96 | −2.18 |
| P4 | 0.06 | −0.01 | 0.67 | 2.09 | 0.01 | 46.10 | 33.14 | 41.04 | −22.09 | 36.62 | 4.14 | 2.16 |
| Increase and decrease in streamflow ($m^3/s$) under RCP 8.5 | | | | | | | | | | | | |
| P1 | −0.71 | −0.64 | −0.50 | −0.32 | −0.18 | 39.99 | 86.77 | 94.73 | −15.07 | −19.97 | 4.03 | −3.43 |
| P2 | −1.08 | −0.37 | −0.06 | −0.13 | 1.05 | 76.99 | 83.03 | 88.07 | 39.44 | −52.62 | 8.51 | −2.93 |
| P3 | −0.05 | 1.49 | −0.01 | −0.08 | −0.10 | 85.56 | 81.23 | 96.72 | 34.05 | −8.47 | 31.60 | −1.66 |
| P4 | −0.24 | 0.56 | 3.38 | 0.85 | −0.06 | 89.55 | 87.35 | 93.08 | −19.24 | 68.99 | 7.61 | −1.70 |

(b)

| Month | Jan | Feb | Mar | Apr | May | Jun | Jul | Aug | Sep | Oct | Nov | Dec |
|---|---|---|---|---|---|---|---|---|---|---|---|---|
| Base period streamflow (B_flow) ($m^3/s$) | | | | | | | | | | | | |
| (1983–2005) | 6.34 | 4.43 | 2.76 | 1.27 | 0.44 | 88.68 | 187.77 | 213.38 | 296.73 | 159.23 | 16.16 | 11.05 |
| Increase and decrease in streamflow ($m^3/s$) under RCP4.5 | | | | | | | | | | | | |
| P1 | 0.86 | 0.64 | 0.55 | 0.67 | 0.76 | 48.58 | 9.19 | 24.77 | 23.57 | −29.24 | −1.96 | −0.76 |
| P2 | 1.16 | 0.88 | 0.81 | 1.03 | 0.98 | 54.69 | 19.02 | 44.71 | 29.16 | −59.74 | 4.44 | −0.27 |
| P3 | 0.76 | 0.62 | 0.64 | 0.99 | 1.02 | 60.34 | 22.59 | 42.54 | 20.36 | −34.63 | 1.57 | −0.45 |
| P4 | 1.76 | 1.48 | 1.29 | 1.33 | 1.15 | 57.22 | 33.60 | 39.65 | 9.10 | −37.28 | 12.78 | 0.21 |
| Increase and decrease in streamflow ($m^3/s$) under RCP 8.5 | | | | | | | | | | | | |
| P1 | 0.33 | 0.23 | 0.27 | 0.55 | 0.69 | 79.08 | 40.55 | 75.91 | 29.77 | −41.11 | −2.00 | −0.91 |
| P2 | 1.02 | 0.76 | 0.74 | 0.89 | 0.96 | 108.27 | 67.98 | 86.01 | 43.28 | −98.67 | −1.53 | −1.07 |
| P3 | 1.19 | 0.92 | 0.90 | 1.06 | 0.99 | 119.05 | 80.43 | 87.30 | 59.78 | −87.71 | 2.06 | −0.34 |
| P4 | 2.73 | 2.14 | 1.81 | 1.84 | 1.43 | 115.94 | 72.33 | 92.78 | 14.17 | −54.72 | 21.10 | 2.52 |

and 8.57–16.93% (183.38 to 330.11 $m^3/s$), under RCP 4.5 and RCP 8.5. In spite of the average annual increase in streamflow, considerable changes in monthly average streamflow have been observed. The model MPI-CSC-REMO2009 and IITM-RegCM4-1 represents similar streamflow output. However, average monthly streamflow for MPI-CSC-REMO2009, SMHI-RCA4 and IITM-RegCM4-1 ranges from P1 (−29.24 to 50.64 $m^3/s$), P2 (−59.74 to 54.69 $m^3/s$), P3 (−34.62 to 60.33 $m^3/s$) and P4 (−37.27 to 57.21 $m^3/s$) under RCP 4.5 and P1 (−41.11 to 94.72 $m^3/s$), P2 (−98.67 to 108.27 $m^3/s$), P3 (−87.70 to 119.05 $m^3/s$) and P4 (−54.71 to 115.94 $m^3/s$) under RCP 8.5. Where, a negative value indicates a decrease in the streamflow. The analysis indicates monthly average streamflow has been increased in wet season for all the models whereas in the dry season there has been no major changes for both the scenario. The change in streamflow is depicted in the following Table 3.

### 3.6. Climate change impact on sediment concentration

The SWAT result shows an increase in average annual sediment concentration in the Purna river basin. The average annual sediment concentration with linear scaling increased by 1.36–15.99% (28.69 to 337.13 mg/l) and 2.23–14.90% (76.55 to 701.53 mg/l) under RCP 4.5 and RCP8.5.The average monthly sediment concentration for MPI-CSC-REMO2009, SMHI-RCA4 and IITM-RegCM4–1 ranges from P1 (−25.38 to 64.78 mg/l), P2 (−58.50 to 91.81 mg/l), P3 (−7.30 to 93.35 mg/l) and P4(−7.30 to 96.66 mg/l) under RCP 4.5 and P1 (−69.22 to138.96 mg/l), P2 (−124.00 to178.03 mg/l), P3 (−7.30 to 152.72 mg/l) and P4 (−5.63 to162.96 mg/l) under RCP 8.5 depicted in Table 4. The result indicates larger portion sediment transported in the wet season. A negative value indicates a decrease in sediment transport, especially in dry season. The change in monthly average sediment concentration is depicted in the Fig. 6 (b).

## 4. Discussion

The Purna river is an important source for agriculture, ecosystem and drinking water supply in the Maharashtra regions. Hence, streamflow, sediment concentration and climate change evaluation are the crucial issues in the basin. In this study, SWAT is used to assess the impact of climate change on streamflow and sediment concentration. As per the guidelines given in Abbaspour et al. (2015) the SWAT general execution in terms of statistical indices such as ($R^2$ and $E_{NS}$) can be judged as good, particularly considering constrained information conditions in the basin. However, the model performance shows the satisfactory agreement between observed and simulated values. Calibration and validation results are varying between $R^2$ (0.71 to 0.91) and $E_{NS}$ (0.65 to 0.91) for streamflow and sediment concentration. Furthermore, climate change impact on these processes has been analyzed using projected precipitation and temperature under RCP 4.5 and RCP 8.5. The SWAT projected precipitation indicate increasing trend, especially in the wet season whereas the increase in temperature is observed in the dry season. It is noticed that, streamflow and sediment concentration are expected to increase measurably under RCP 8.5 for the future time period. The similar trends were found by Mishra and Lilhare (2016), the streamflow during the wet season was projected to increase in the majority of the sub-continental river basin. The increase in monthly streamflow in the Purna river basin varies from (24.47 to57.22 $m^3/s$) and (39.99 to 115.94 $m^3/s$) under RCP 4.5 and RCP 8.5. Whereas, increase in precipitation also leads to sediment concentration in the river basin which, varies from (32.58 to 96.66 mg/l) and (68.43 to 162.96 mg/l) under RCP 4.5 and RCP 8.5. The results clearly indicate the climate change impact on the basin. Additionally, no indicative linear relationship is identified among streamflow/sediment and temperature. This stipulates that although the study shows warmer climate projection, the change of temperature does not account for the inter-annual

**Table 4**
Predicted relative change in monthly sediment concentration with the base period under RCP 4.5 and RCP 8.5 for (a) MPI-CSC-REMO2009 model and IITM-RegCM4-1 model (b) SMHI-RCA4 model.

(a)

| Month | Jan | Feb | Mar | Apr | May | Jun | Jul | Aug | Sep | Oct | Nov | Dec |
|---|---|---|---|---|---|---|---|---|---|---|---|---|
| Base period sediment concentration (sed) (mg/l) | | | | | | | | | | | | |
| (1983–2005) | 5.29 | 2.91 | 4.14 | 7.30 | 4.12 | 336.47 | 536.85 | 443.06 | 484.18 | 253.98 | 25.44 | 4.67 |
| Increase and decrease in sediment concentration (sed) (mg/l) RCP4.5 | | | | | | | | | | | | |
| P1 | −4.01 | 3.25 | −4.14 | 2.43 | −4.12 | 63.30 | 51.40 | 46.28 | −57.30 | −58.51 | −9.13 | −0.78 |
| P2 | 1.08 | −0.19 | −1.13 | −6.04 | −4.12 | 63.62 | 53.36 | 91.81 | −58.50 | −41.29 | 0.36 | 2.06 |
| P3 | −0.09 | −0.74 | −1.58 | −2.63 | −4.12 | 64.44 | 43.41 | 32.58 | 31.40 | 41.97 | −7.79 | −1.43 |
| P4 | −0.66 | −0.24 | −0.18 | −2.79 | −3.89 | 35.68 | 37.11 | 65.59 | 63.92 | 49.39 | −7.04 | 2.41 |
| Increase and decrease in sediment concentration (sed) (mg/l) RCP 8.5 | | | | | | | | | | | | |
| P1 | 0.11 | 2.29 | −4.14 | −7.30 | −4.12 | 82.63 | 92.30 | 95.58 | −106.72 | −69.22 | −5.18 | 0.32 |
| P2 | 2.26 | 1.82 | 1.51 | −6.30 | −3.03 | 103.49 | 139.01 | 178.03 | −124.00 | −72.99 | 11.98 | 7.35 |
| P3 | 2.10 | −0.15 | −4.02 | −3.70 | −4.12 | 122.18 | 103.83 | 82.19 | 99.65 | 71.97 | 11.39 | 0.26 |
| P4 | 0.03 | −1.20 | −2.38 | −1.21 | −4.12 | 78.41 | 68.43 | 142.28 | 149.03 | 108.12 | 8.73 | 3.37 |

(b)

| Month | Jan | Feb | Mar | Apr | May | Jun | Jul | Aug | Sep | Oct | Nov | Dec |
|---|---|---|---|---|---|---|---|---|---|---|---|---|
| Base period sediment (sed) (mg/l) | | | | | | | | | | | | |
| (1983–2005) | 5.29 | 2.91 | 4.14 | 7.30 | 4.12 | 336.47 | 536.85 | 443.06 | 484.18 | 253.98 | 25.44 | 4.67 |
| Increase and decrease in sediment concentration (sed) (mg/l) RCP4.5 | | | | | | | | | | | | |
| P1 | −5.29 | −2.91 | −4.14 | −7.30 | −4.12 | 59.02 | 28.45 | 57.13 | 64.78 | −25.38 | 10.76 | −0.89 |
| P2 | −5.29 | −2.91 | −4.14 | −7.30 | −4.12 | 77.53 | 33.88 | 71.58 | 59.61 | −32.65 | 11.68 | 0.67 |
| P3 | −5.29 | −2.91 | −4.14 | −7.30 | −4.12 | 74.33 | 42.97 | 93.35 | 76.47 | −3.94 | 4.99 | −1.77 |
| P4 | −5.29 | −2.91 | −4.14 | −7.30 | −4.12 | 72.05 | 54.35 | 96.66 | 95.06 | 25.03 | 22.42 | −4.67 |
| Increase and decrease in sediment concentration (sed) (mg/l) RCP 8.5 | | | | | | | | | | | | |
| P1 | −5.29 | −2.91 | −4.14 | −7.30 | −4.12 | 126.93 | 99.67 | 100.82 | 138.96 | −57.64 | 13.18 | −4.24 |
| P2 | −5.29 | 2.91 | −4.14 | −7.30 | −4.12 | 131.78 | 108.56 | 135.06 | 154.32 | −23.43 | 17.18 | 0.36 |
| P3 | −5.29 | −2.91 | −4.14 | −7.30 | −4.12 | 127.53 | 117.48 | 152.72 | 146.53 | 38.18 | 15.54 | −1.03 |
| P4 | −5.29 | −2.91 | −4.14 | −5.63 | −4.12 | 159.09 | 136.66 | 162.96 | 162.13 | 52.66 | 54.67 | −4.54 |

variations of streamflow and sediment concentration. Increase in average precipitation may lead to change in the frequency and intensity of the events like a flood. Moreover, intense rainfall is expected in future time with a decrease in number of rainy days. Coupled with these, decrease in rainfall in summer may put additional water demand particularly for agriculture and drinking. Hence some preventive measures such as early warning system, development of flood prone areas provision of safe drinking water, reservoir safety must necessarily be considered. Similarly to cope up with water availability adaptation measures such as improvement in irrigation efficiency, optimal reservoir operation policy, development of water harvesting schemes, water demand management may be useful. A general increase in sediment concentration may bring out on forefront issues such as erosion vulnerability, water quality issue, siltation of water ways and excess cost for the water treatment in the basin. Considering future water availability in the basin, the rise of vegetation cover could be implemented as soil conservation measures. The projected climate change may also induce extra stress on various adoption strategies such as land use land cover change, water distribution, cropping pattern, flood warning system *etc.* and required precise integrated analysis before policy decision. Further, the uncertainties involved in the GHG emission scenario, climatic model, bias correction technique, hydrological model are the limitations of the study. Hence to examine uncertainty and enhance the climate data precision will be one of the essential objective of our future work.

## 5. Conclusion

The study discerned the impacts of climate change on streamflow and sediment concentration in the Purna river basin. The SWAT model coupled with the SUFI-2 algorithm is used for the calibration, validation, sensitivity and uncertainty analysis. The parameters, namely ALPHA_BNK, SOL_K, CN2, ALPHA_BF, CH_K2 are found as the most sensitive parameters. Two climate projections RCP 4.5 and RCP 8.5 are selected for the period of P1 (2009–2031), P2 (2032–2053), P3 (2054–2075) and P4 (2076–2099). The RCP 8.5 extreme scenario shows that average temperature of the basin is supposed to increase by range 0.52–1.32 °C. Similarly, average precipitation in the basin is expected to increase by range 4.90–10.61%. Monthly variations indicate that increase in streamflow and sediment concentration is more predominant in the wet season. The monthly average streamflow varies significantly throughout the year and relatively high in June, July, August and September. The study also indicates that the stream contributes more than 50% of sediment concentration by eroding stream bank and deposit sediment in the watershed. Projected climate change results indicate, there does not appear to be a problem of water availability, especially in a wet season by this century. Finally, results revealed that SWAT is capable of simulating long-term climate impact studies and can be utilized to develop an effective strategy for a sustainable improvement of the water resources in Purna river basin.

## Acknowledgment

Authors are thankful to (TEQIP, DST-FIST) Government of India and authorities of SGGS IE &T for providing workstation and valuable guidance for completing the work.

## Appendix A. Supplementary data

Supplementary data to this article can be found online at https://doi.org/10.1016/j.scitotenv.2018.09.334.

## References

Abbaspour, K.C., Rouholahnejad, E., Vaghefi, S., Srinivasan, R., Yang, H., Kløve, B., 2015. A continental-scale hydrology and water quality model for Europe: calibration and uncertainty of a high-resolution large-scale SWAT model. J. Hydrol. 524, 733–752.

Abdo, K.S., Fiseha, B.M., Rientjes, T.H.M., Gieske, A.S.M., Haile, A.T., 2009. Assessment of climate change impacts on the hydrology of Gilgel Abay catchment in Lake Tana basin, Ethiopia. Hydrol. Process. 23, 3661–3669.

Anand, J., Gosain, A.K., Khosa, R., 2018. Prediction of land use changes based on Land Change Modeler and attribution of changes in the water balance of Ganga basin to land use change using the SWAT model. Sci. Total Environ. 644, 503–519.

Arnell, N.W., 1999. Climate change and global water resources. Glob. Environ. Chang. 9, 31–49.

Arnold, J.G., Moriasi, D.N., Gassman, P.W., Abbaspour, K.C., White, M.J., Srinivasan, R., Santhi, C., Harmel, R.D., Griensven, Van, a., VanLiew, M.W., Kannan, N., Jha, M.K., 2012. Swat: Model Use, Calibration, and Validation. 55. Asabe, pp. 1491–1508 (https://doi.org/ISSN 2151-0032).

Bajracharya, A.R., Bajracharya, S.R., Shrestha, A.B., Maharjan, S.B., 2018. Climate change impact assessment on the hydrological regime of the Kaligandaki Basin, Nepal. Sci. Total Environ. 625, 837–848.

Baker, T.J., Miller, S.N., 2013. Using the Soil and Water Assessment Tool (SWAT) to assess land use impact on water resources in an East African watershed. J. Hydrol. 486, 100–111.

Bharati, L., Gurung, P., Jayakody, P., 2012. Hydrologic characterization of the Koshi Basin and the impact of climate change. Hydro Nepal J. Water, Energy Environ. 11, 18–22.

Chaibou Begou, J., Jomaa, S., Benabdallah, S., Bazie, P., Afouda, A., Rode, M., 2016. Multi-site validation of the SWAT model on the Bani catchment: model performance and predictive uncertainty. WaterSA 8, 1–23.

Christensen, N.S., Wood, A.W., Voisin, N., Lettenmaier, D.P., Palmer, R.N., 2004. The effects of climate change on the hydrology and water resources of the Colorado River basin. Clim. Chang. 62, 337–363.

Cousino, L.K., Becker, R.H., Zmijewski, K.A., 2015. Modeling the effects of climate change on water, sediment, and nutrient yields from the Maumee River watershed. J. Hydrol. Reg. Stud. 4, 762–775.

Dahal, V., Shakya, N.M., Bhattarai, R., 2016. Estimating the impact of climate change on water availability in Bagmati Basin, Nepal. Environ. Process. 3, 1–17.

Das, J., Umamahesh, N.V., 2016. Downscaling monsoon rainfall over river Godavari Basin under different climate-change scenarios. Water Resour. Manag. 30, 5575–5587.

Delpla, I., Jung, A.-V., Baures, E., Clement, M., Thomas, O., 2009. Impacts of climate change on surface water quality in relation to drinking water production. Environ. Int. 35, 1225–1233.

Di Baldassarre, G., Elshamy, M., van Griensven, A., Soliman, E., Kigobe, M., Ndomba, P., Mutemi, J., Mutua, F., Moges, S., Xuan, Y., et al., 2011. Future hydrology and climate in the River Nile basin: a review. Hydrol. Sci. J. 56, 199–211.

Faramarzi, M., Abbaspour, K.C., Vaghefi, S.A., Farzaneh, M.R., Zehnder, A.J.B., Srinivasan, R., Yang, H., 2013. Modeling impacts of climate change on freshwater availability in Africa. J. Hydrol. 480, 85–101.

Fereidoon, M., Koch, M., 2018. SWAT-MODSIM-PSO optimization of multi-crop planning in the Karkheh River Basin, Iran, under the impacts of climate change. Sci. Total Environ. 630, 502–516.

Ficklin, D.L., Luo, Y., Luedeling, E., Zhang, M., 2009. Climate change sensitivity assessment of a highly agricultural watershed using SWAT. J. Hydrol. 374, 16–29. https://doi.org/10.1016/j.jhydrol.2009.05.016.

Gosain, a K., Rao, S., Basuray, D., 2006. Climate change impact assessment on hydrology of Indian river basins. Current 90, 346–353.

Gupta, P.K., Punalekar, S., Panigrahy, S., Sonakia, A., Parihar, J.S., 2011. Runoff modeling in an agro-forested watershed using remote sensing and GIS. J. Hydrol. Eng. 17, 1255–1267.

Hosseini, R., Newlands, N.K., Dean, C.B., Takemura, A., 2015. Statistical modeling of soil moisture, integrating satellite remote-sensing (SAR) and ground-based data. Remote Sens. 7, 2752–2780.

Johnston, R., Smakhtin, V., 2014. Hydrological modeling of large river basins: how much is enough? Water Resour. Manag. 28, 2695–2730.

Joo, J., Zhang, A., Li, X., Zheng, C., 2017. Hydrological responses to climate shifts for a minimally disturbed mountainous watershed in northwestern China. Hydrol. Sci. J. 62, 1440–1455.

Lenderink, G., Buishand, A., van Deursen, W., 2007. Estimates of future discharges of the river Rhine using two scenario methodologies: direct versus delta approach. Hydrol. Earth Syst. Sci. 11, 1145–1159.

Li, T., Gao, Y., 2015. Runoff and sediment yield variations in response to precipitation changes: a case study of Xichuan watershed in the loess plateau, China. WaterSA 7, 5638–5656.

Ligaray, M., Kim, H., Sthiannopkao, S., Lee, S., Cho, K.H., Kim, J.H., 2015. Assessment on hydrologic response by climate change in the Chao Phraya River basin, Thailand. WaterSA 7, 6892–6909. https://doi.org/10.3390/w7126665.

Lindner, M., Maroschek, M., Netherer, S., Kremer, A., Barbati, A., Garcia-Gonzalo, J., Seidl, R., Delzon, S., Corona, P., Kolström, M., et al., 2010. Climate change impacts, adaptive capacity, and vulnerability of European forest ecosystems. For. Ecol. Manag. 259, 698–709.

Malagó, A., Bouraoui, F., Vigiak, O., Grizzetti, B., Pastori, M., 2017. Modelling water and nutrient fluxes in the Danube River Basin with SWAT. Sci. Total Environ. 603, 196–218.

McGuire, A.D., Sitch, S., Clein, J.S., Dargaville, R., Esser, G., Foley, J., Heimann, M., Joos, F., Kaplan, J., Kicklighter, D.W., et al., 2001. Carbon balance of the terrestrial biosphere in the twentieth century: analyses of $CO_2$, climate and land use effects with four process-based ecosystem models. Glob. Biogeochem. Cycles 15, 183–206.

Meng, Y., Zhou, L., He, S., Lu, C., Wu, G., Ye, W., Ji, P., 2018. A heavy metal module coupled with the SWAT model and its preliminary application in a mine-impacted watershed in China. Sci. Total Environ. 613, 1207–1219.

Min, S.-K., Zhang, X., Zwiers, F.W., Hegerl, G.C., 2011. Human contribution to more-intense precipitation extremes. Nature 470, 378–381.

Mishra, V., Lilhare, R., 2016. Hydrologic sensitivity of Indian sub-continental river basins to climate change. Glob. Planet. Chang. 139, 78–96.
Murty, P.S., Pandey, A., Suryavanshi, S., 2014. Application of semi-distributed hydrological model for basin level water balance of the Ken basin of Central India. Hydrol. Process. 28, 4119–4129.
Nilawar, A.P., Calderella, C.P., Lakhankar, T.Y., Waikar, M.L., Munoz, J., 2017. Satellite soil moisture validation using hydrological SWAT model: a case study of Puerto Rico, USA. Hydrology 4, 1–11.
Romagnoli, M., Portapila, M., Rigalli, A., Maydana, G., Burgués, M., García, C.M., 2017. Assessment of the SWAT model to simulate a watershed with limited available data in the Pampas region, Argentina. Sci. Total Environ. 596, 437–450.
Routschek, A., Schmidt, J., Kreienkamp, F., 2014. Impact of climate change on soil erosion a high-resolution projection on catchment scale until 2100 in Saxony/Germany. Catena 121, 99–109.
Shi, P., Hou, Y., Xie, Y., Chen, C., Chen, X., Li, Q., Qu, S., Fang, X., Srinivasan, R., 2013. Application of a SWAT model for hydrological modeling in the Xixian Watershed, China. J. Hydrol. Eng. 18, 1522–1529.
Tan, M.L., Ficklin, D.L., Yusop, Z., et al., 2014. Impacts and uncertainties of climate change on streamflow of the Johor River Basin, Malaysia using a CMIP5 General Circulation Model ensemble. J. Water Clim. Chang. 5, 676–695.
Teutschbein, C., Seibert, J., 2012. Bias correction of regional climate model simulations for hydrological climate-change impact studies: review and evaluation of different methods. J. Hydrol. 456, 12–29.
Tuo, Y., Duan, Z., Disse, M., Chiogna, G., 2016. Evaluation of precipitation input for SWAT modeling in alpine catchment: a case study in the Adige river basin (Italy). Sci. Total Environ. 573, 66–82.
Van Vuuren, D.P., Edmonds, J., Kainuma, M., Riahi, K., Thomson, A., Hibbard, K., Hurtt, G.C., Kram, T., Krey, V., Lamarque, J.-F., et al., 2011. The representative concentration pathways: an overview. Clim. Chang. 122, 415–429.
Vigiak, O., Malagó, A., Bouraoui, F., Vanmaercke, M., Obreja, F., Poesen, J., Habersack, H., Fehér, J., Grošelj, S., 2017. Modelling sediment fluxes in the Danube River Basin with SWAT. Sci. Total Environ. 599, 992–1012.
Willems, P., Vrac, M., 2011. Statistical precipitation downscaling for small-scale hydrological impact investigations of climate change. J. Hydrol. 402, 193–205.
Williams, J.R., Kannan, N., Wang, X., Santhi, C., Arnold, J.G., 2011. Evolution of the SCS runoff curve number method and its application to continuous runoff simulation. J. Hydrol. Eng. 17, 1221–1229.
Xue, C., Chen, B., Wu, H., 2013. Parameter uncertainty analysis of surface flow and sediment yield in the Huolin Basin, China. J. Hydrol. Eng. 19, 1224–1236.
Yang, J., Reichert, P., Abbaspour, K.C., Xia, J., Yang, H., 2008. Comparing uncertainty analysis techniques for a SWAT application to the Chaohe Basin in China. J. Hydrol. 358, 1–23.
Zeiger, S.J., Hubbart, J.A., 2016. A SWAT model validation of nested-scale contemporaneous stream flow, suspended sediment and nutrients from a multiple-land-use watershed of the central USA. Sci. Total Environ. 572, 232–243.
Zhang, X., Srinivasan, R., Hao, F., 2007. Predicting hydrologic response to climate change in the Luohe River basin using the SWAT model. Trans. ASABE 50, 901–910.
Zhao, G., Mu, X., Jiao, J., Gao, P., Sun, W., Li, E., Wei, Y., Huang, J., 2018. Assessing response of sediment load variation to climate change and human activities with six different approaches. Sci. Total Environ. 639, 773–784.